Biochemistry and Molecular Biology

Allele-Specific Inhibition of Rhodopsin With an Antisense Oligonucleotide Slows Photoreceptor Cell Degeneration

Susan F. Murray,[1] Ali Jazayeri,[1] Michael T. Matthes,[2] Douglas Yasumura,*,[2] Haidong Yang,[2] Raechel Peralta,[1] Andy Watt,[1] Sue Freier,[1] Gene Hung,[1] Peter S. Adamson,[3] Shuling Guo,[1] Brett P. Monia,[1] Matthew M. LaVail,[2] and Michael L. McCaleb[1]

[1]Isis Pharmaceuticals, Carlsbad, California, United States
[2]University of California at San Francisco School of Medicine, Beckman Vision Center, San Francisco, California, United States
[3]GlaxoSmithKlein, Brentford, Middlesex, United Kingdom

PURPOSE. To preserve photoreceptor cell structure and function in a rodent model of retinitis pigmentosa with P23H *rhodopsin* by selective inhibition of the mutant *rhodopsin* allele using a second generation antisense oligonucleotide (ASO).

METHODS. Wild-type mice and rats were treated with ASO by intravitreal (IVT) injection and *rhodopsin* mRNA and protein expression were measured. Transgenic rats expressing the murine *P23H rhodopsin* gene (P23H transgenic rat Line 1) were administered either a mouse-specific P23H ASO or a control ASO. The contralateral eye was injected with PBS and used as a comparator control. Electroretinography (ERG) measurements and analyses of the retinal outer nuclear layer were conducted and correlated with *rhodopsin* mRNA levels.

RESULTS. *Rhodopsin* mRNA and protein expression was reduced after a single ASO injection in wild-type mice with a *rhodopsin-specific* ASO. Transgenic rat eyes that express a murine P23H rhodopsin gene injected with a murine P23H ASO had a 181 ± 39% better maximum amplitude response (scotopic a-wave) as compared with contralateral PBS-injected eyes; the response in control ASO eyes was not significantly different from comparator contralateral eyes. Morphometric analysis of the outer nuclear layer showed a significantly thicker nuclear layer in eyes injected with murine P23H ASO (18%) versus contralateral PBS-injected eyes.

CONCLUSIONS. Allele-specific ASO-mediated knockdown of mutant P23H *rhodopsin* expression slowed the rate of photoreceptor degeneration and preserved the function of photoreceptor cells in eyes of the P23H *rhodopsin* transgenic rat. Our data indicate that ASO treatment is a potentially effective therapy for the treatment of retinitis pigmentosa.

Keywords: rhodopsin, antisense, allele-specific, adRP

Retinitis pigmentosa (RP) is a hereditary degenerative disease that typically causes blindness by middle age.[1–3] Over 100 rhodopsin mutations have been identified in patients with RP; the predominant autosomal dominant mutation in the United States is P23H.[4,5] The P23H mutation is present in approximately 25% of autosomal dominant (adRP) and 5% to 15% of RP cases (available in the public domain at https://sph.uth.tmc.edu/Retnet).[4,6,7] A number of strategies are under evaluation for the treatment of ocular diseases, but few are targeted at autosomal dominant diseases and involve allele-selective inhibition of protein expression. The therapeutic approaches to date have involved the addition of neurotrophic factors,[8] gene suppression and replacement,[9,10] modifications of survival and chaperone pathways,[11] and correction of the mutation at the DNA level.[12] Most strategies using the gene silencing approach are allele nonselective and are being used in combination with gene therapy. The inhibitors under investigation include small catalytic RNAs (ribozymes),[13,14] short interfering RNAs (siRNAs, shRNA),[10,12,15] and zinc finger–based transcriptional repressors,[16] all requiring a delivery vehicle, such as adeno-associated virus (AAV) vectors, for effectiveness.[17,18,14] Ribozyme technology has the potential to discriminate between mutant and wild-type sequences, but no commercial ribozymes have been marketed despite considerable effort.[12,19,20] In dominant negative diseases, such as P23H adRP, data suggest that significant phenotypic improvements can result from modest reductions in the mutant protein when wild-type protein expression is preserved.[20,21] A therapeutic strategy involving reduction of the mutant rhodopsin RNA allele and maintaining wild-type (WT) rhodopsin (RHO), in adRP patients is supported by transgenic rodent studies in demonstrating functional improvements in photoreceptor cells after RNA silencing treatments.[20,22] Lewin et al.[22] demonstrated that small reductions (~15%) in mutant rhodopsin RNA levels in transgenic rats slowed the rate of photoreceptor degeneration. This study was the first demonstration of functional preservation of retinal degeneration through a gene silencing mechanism. In another study using the same ribozyme construct, LaVail et al.[20] demonstrated similar results after introducing the treatment at a much later time in disease progression, which is more similar to what would be experienced in RP patients.

In this report, we tested an allele-specific approach in a rodent model of adRP with antisense technology. Second generation antisense oligonucleotides (ASOs) have the potential to selectively silence an allele with a single base pair difference

Investigative Ophthalmology & Visual Science

from the normal allele[23] and have several advantages when compared with other gene silencing agents. First, ASO can be delivered in a water-based formulation with no delivery system required.[24] Second, therapeutic doses of ASOs can be administered by intravitreal (IVT) injections that result in little to no systemic exposure.[24,25] Third, Ostergaard et al.[26] demonstrated when targeting a single base mutation, position-dependent chemical modifications to the ASO can provide substantial selectivity between alleles, making mutation-specific, allele-dependent targeting a viable approach. They demonstrated discrimination for a single nucleotide change in the disease-causing huntingtin mRNA, in patient cells and in a humanized mouse model of Huntington disease. These findings suggest that efficient allele-selective down regulation of gene expression using ASOs can be applied to other dominant genetic disorders, such as P23H adRP.[26] Furthermore, IVT administration of ASOs is a clinically validated approach with good tolerability and duration of action that provides acceptable patient safety and convenience.[27,28]

To demonstrate the efficacy of an allele-selective antisense treatment we chose a transgenic rat model of RP, the P23H rat Line 1 (P23H-1). This transgenic rat carries the mutant mouse rhodopsin gene in addition to the endogenous wild-type rat rhodopsin gene leading to the onset of photoreceptor cell death as early as the second postnatal week.[29] Machida et al.[30] carefully evaluated this P23H-1 transgenic rat model of RP and showed a rapidly progressive rod dysfunction, with initial normal cone function.[31] This finding is consistent with clinical findings reported in human P23H adRP patients.[32] However, differences were noted in the rate of recovery from a light bleach and in transduction sensitivity from a-wave modeling compared with human adRP patients.[30,32] Despite these differences, the P23H transgenic rats are considered one of the best models of adRP to evaluate potential therapeutic treatments.[29,30] In this report, we evaluated the effects of an allele-selective antisense compound on the retinal degeneration in the P23H-1 rat line. This compound is a mouse-specific P23H *rhodopsin* ASO and was administered by IVT injection. We showed that the P23H *rhodopsin* ASO specifically reduced mutant mouse *rhodopsin* gene expression without altering expression of the normal rat *rhodopsin* gene. In rhodopsin ASO-treated eyes, we demonstrated better photoreceptor cell function and viability without overt toxicities or inflammatory side effects.

MATERIALS AND METHODS

Oligonucleotides

Antisense oligonucleotides were designed and synthesized using an Applied Biosystems 380B automated DNA synthesizer (PerkinElmer Life and Analytical Sciences–Applied Biosystems, Waltham, MA, USA) and purified as previously described.[23]

mRHO ASO1; targets exon 5 (5′-<u>AGCTA</u>CTATGTGTTC<u>CATTC</u>-3′),

mRHO ASO3; targets exon 5 (5′-<u>CTGGT</u>ACCCCA TAGTT<u>CCTG</u>-3′),

MALAT1 ASO (5′-<u>GGGTC</u>AGCTGCCAAT<u>GCTAG</u>-3′), and Control ASO

(5′-<u>CCTTC</u>CCTGAAGGTT<u>CCTCC</u>-3′) are chimeric 20-mers with phosphorothioate backbone containing 2′-O-methoxyethyl (MOE) modification at positions 1-5 and 15-20 (second generation chemistry; Isis Pharmaceuticals, Carlsbad, CA, USA). mRHO ASO2 targets exon 5 (5′-<u>ATGAGG</u> CAAGGTT<u>TCC</u>-3′) is a chimeric 16-mer phosphorothioate oligonucleotide containing constrained ethyl (cEt) modification at positions 1 to 3 and 14 to 16 (Table), which was synthesized and purified on an automated DNA synthesizer using phosphoramidite chemistry as previously described.[33]

TABLE. Description of Antisense Oligonucleotides

ASO ID	Complementary Gene	Species	Pharmacologic Use
MALAT ASO	*Malat 1*	Mouse	Used to evaluate activity in all ocular layers
Control ASO	None	None	Control ASO with no known gene sequence homology
mRHO ASO1	*Rhodopsin*	Mouse	Characterization of activity in photoreceptor cells
mRHO ASO2	*Rhodopsin*	Mouse	Confirm activity effects and established duration of action
mRHO ASO3	*Rhodopsin*	Mouse	Mouse-specific sequence with no activity in rat used for transgenic pharmacology studies

Animals

In vivo studies in wild-type animals were performed with 6-week-old male C57BL/6 mice from Jackson Laboratories (Sacramento, CA, USA) or male Sprague-Dawley rats from Charles River Laboratories (San Diego, CA, USA), according to the indicated treatment schedules. The animals were housed in microisolator cages on a constant 12-hour light-dark cycle. Transgenic rats with a P23H *rhodopsin* mutation (produced by Chrysalis DNX Transgenic Sciences, Princeton, NJ, USA) on an albino Sprague-Dawley background, P23H Transgenic Line 1 (abbreviated P23H-1) were reared and maintained in a 12 hour light–dark environment. The experimental rats were produced by crossing transgenic homozygotes by Sprague-Dawley rats; the P23H-1 hemizygotes have nine copies of the transgene.[34] All procedures were approved by the Institutional Animal Care and Use Committees (Isis Pharmaceuticals and University of California at San Francisco, San Francisco, CA, USA) and adhered to the ARVO Statement for the Use of Animals in Ophthalmic and Vision Research.

Intravitreal Injections

For intravitreal injections in wild-type animals, each eye was treated with a drop of 0.5% Tropicamide ophthalmic solution to open iris and a drop of Proparacaine hydrochloride (0.5% ophthalmic solution) to inhibit eye twitching. One microliter of PBS or ASO was injected into the vitreous using a 33-G needle under a dissecting microscope. Necropsy was performed by cardiac puncture from animals anesthetized by inhaled 1% to 3% isoflurane and whole eyes removed and processed for either RNA or histologic analysis. For P23H-1 rats, animals were anesthetized with intramuscular injections of xylazine (13 mg/kg) and ketamine (87 mg/kg). Prior to IVT injection 2.5% phenylephrine was used to dilate the pupils and then the topical anesthetic, Proparacaine, was applied. Under a dissecting microscope, all rats had 2 μL PBS injected in the left eye as a "surgical" control, and the right eye received 2 μL either mRHO ASO3 or Control ASO, using a 32-G needle.

Histologic Analysis

Hematoxylin and Eosin Staining. One set of paraffin-embedded tissue sections were deparaffinized and stained with hematoxylin and eosin (Surgpath; Leica Biosystems, Buffalo Grove, IL, USA).

Immunohistochemical Analysis. Tissue sections were collected, fixed in Davidson's solution, and paraffin embedded. Sections were stained using a polyclonal rabbit anti-ASO antibody (Isis Pharmaceuticals) for ASO uptake as previously described.[35,36]

ViewRNA Assay (ISH). *MALAT1* expression was detected using the QuantiGene_ViewRNA tissue assay (Cat. #QVT0011; Affymetrix, Santa Clara, CA, USA) according to the manufacturer's instructions with optimal conditions as previously described.[35] For the *Rhodopsin* expression mouse-specific rhodopsin probes were purchased from Affymetrix (Cat. #VX1-99999-01; accession #NM_145383). Briefly, rat tissues were fixed in Davidson's solution and embedded into paraffin. After deparaffinization, the tissue slides were boiled for 10 minutes followed by treatment with protease at 40°C for 20 minutes. The rhodopsin RNA probe was used at a 1:40 dilution and was incubated with sample at 40°C for 180 minutes. After washing, the rhodopsin RNA/probe complex was hybridized with preamplifier, amplifier, and AP-oligonucleotides at 40°C. After removal of free AP-oligonucleotide by washing in PBS, the slide was incubated with Fast Red substrate at 40°C for 30 minutes. The tissue images were acquired using an Aperio scanner (Leica Biosystems).

RNA and qRT-PCR Analysis

Whole eyes or retinas were homogenized in a guanidine isothiocyanate solution (Life Technologies, Carlsbad, CA, USA) supplemented with 8% 2-mercaptoethanol (Sigma-Aldrich Corp., St. Louis, MO, USA). Total RNA was prepared according to the PureLink Total RNA Purification Kit (Life Technologies). The qRT-PCR analyses were done using a StepOne Real-Time PCR System (Life Technologies). All primer probe sets were synthesized at Integrated DNA Technologies (IDT) and are as follows:

Mouse *MALAT1*:
Forward: 5′TGGGTTAGAGAAGGCGTGTACTG-3′;
Reverse: 5′-TCAGCGGCAACTGGGAAA-3′; and
Probe: 5′-Fam-CGTTGGCACGACACCTTCAGGGACT-Tamra-3′.
Mouse *Rhodopsin*:
Forward: 5′-CACTCCATGGCTACTTCGTCTTT-3′;
Reverse: 5′-GGGCGATTTCACCTCCAA-3′; and
Probe: 5′-Fam-CTGTAATCTCGAGGGCTTCTTTGCCACA-Tamra-3′.
Mouse *Cone-Rod Homeobox* (CRX):
Forward: 5′-TCTGAGTGGCCCCAATGTG-3′;
Reverse: 5′- CCGCCGCTGCTTCCTA-3′; and
Probe: 5′-Fam-TGCACCAGGCTGTCCCATACTCAAGTG-Tamra-3′.
Rat *Rhodopsin*:
Forward: 5′-AAGGAATGGGTTGGAGCCTCAGAT-3′;
Reverse: 5′- CCCTTGTCCAACATGGCATGAAGA-3′; and
Probe: 5′-Fam-AAAGGGTGCCAGGACCTGGAATGAAA-Tamra-3′.
Rat *Cone-Rod Homeobox* (CRX):
Forward: 5′-AGGCTCGTCCTGCGAAGAG-3′;
Reverse: 5′- GAATCTGAGATGCCCAAAGGAT-3′; and
Probe: 5′-Fam-CATCCCCGAGACCCTCTACAGATGTTTG-Tamra-3.′

Polymerase chain reaction results were normalized to total RNA measure by Quant-iT RiboGreen RNA Reagent (Life Technologies) for the *MALAT1* data and to *CRX* for *rhodopsin*.

Western Analysis

Mouse retinas were homogenized in 1 mL lysis buffer (RIPA) containing a 1:200 dilution of protease cocktail III (EMD Millipore, Billerica, MA, USA). Protein concentrations were determined using the Bio-Rad DC protein assay (Hercules, CA, USA), and 1 µg protein per sample was pooled and loaded onto a 10% tris-glycine SDS gel (Life Technologies). Blots were incubated with a 1:3000 dilution of anti-rhodopsin antibody (1D4, Cat. #SC57432; Santa Cruz, Santa Cruz, CA, USA) followed by a 1:8000 dilution of goat anti-mouse HRP conjugated secondary antibody (EMD Millipore Cat. #12-349), and then detected using ECL Plus Chemiluminescent reagents (GE Healthcare Life Sciences, Pittsburgh, PA, USA). Blots were than stripped with reblot reagent (Cat. #2502; Chemicon, Billerica, MA, USA) and incubated with a 1:1000 dilution of anti–complement factor B antibody (Cat. #A08825; Sigma-Aldrich Corp.).

Electroretinographic Analysis

Rats were dark-adapted overnight and then anesthetized with intramuscular injections of xylazine (13 mg/kg) and ketamine (87 mg/kg) in dim red light.

Full-field scotopic ERGs were elicited with 10-msec flashes of white light, and responses from both eyes were recorded simultaneously by using a UTAS-E 3000 Visual Electrodiagnostic System (LKC Technologies, Gaithersburg, MD, USA) as described.[22] The corneas of the rats were anesthetized with a drop of 0.5% proparacaine hydrochloride, and the pupils were dilated with 1% atropine and 2.5% phenylephrine hydrochloride. Small contact lenses with gold wire loops46 were placed on both corneas with a drop of 2.5% methylcellulose to maintain corneal hydration. A silver wire reference electrode was placed subcutaneously between the eyes, and a ground electrode was placed subcutaneously in the hind leg. To measure scotopic ERG responses, stimuli were presented at intensities from -4.6 to 2.4 log cd sec m^{-2} (see Figs. 4, 7 for specific intensities) at interstimulus intervals ranging from 5 seconds at lowest intensities to 60 seconds at the highest intensity. Responses were amplified at a gain of 4000, filtered between 0.3 to 500 Hz and digitized at a rate of 2000 Hz on two channels. Three responses were averaged at each intensity. To measure photopic responses, the rats were then exposed to a rod-desensitizing adapting light of 29 cd m^{-2} for 10 minutes before responses were recorded to stimuli (Figs. 4, 7; bottom panel, diamond symbols) presented at a rate of 2 Hz; 20 successive flashes were averaged.[37] For quantitative comparison of differences in a-wave and b-wave response amplitudes between the two eyes of individual rats, the values from each stimulus intensity were averaged for each eye of a given animal.

Retinal Tissue Preparation and Morphometry

P23H-1 rats were euthanized on postnatal day 45 by overdose of carbon dioxide inhalation and immediately enucleated and immersed into a mixture of combined aldehydes (2% paraformaldehyde and 2.5% glutaraldehyde). Eyes were bisected, postfixed in osmium tetroxide, and embedded in epoxy resin, and 1-mm thick histologic sections were made along the vertical meridian.[38] The thickness of the outer nuclear layer (ONL) was taken as a measure of photoreceptor number. For each retina, the mean ONL was obtained from 54 measurements taken around the eye; these values were used for statistical analysis, and groups of three measurements in each 440-µm microscopic field were averaged and the data were plotted as a retinal spidergram to show specific regional differences, as described.[39,40]

Statistical Analyses

Data are presented as means ± SD or ± SEM. One-way ANOVA followed by a Tukey's post hoc tests, 2-way ANOVA followed
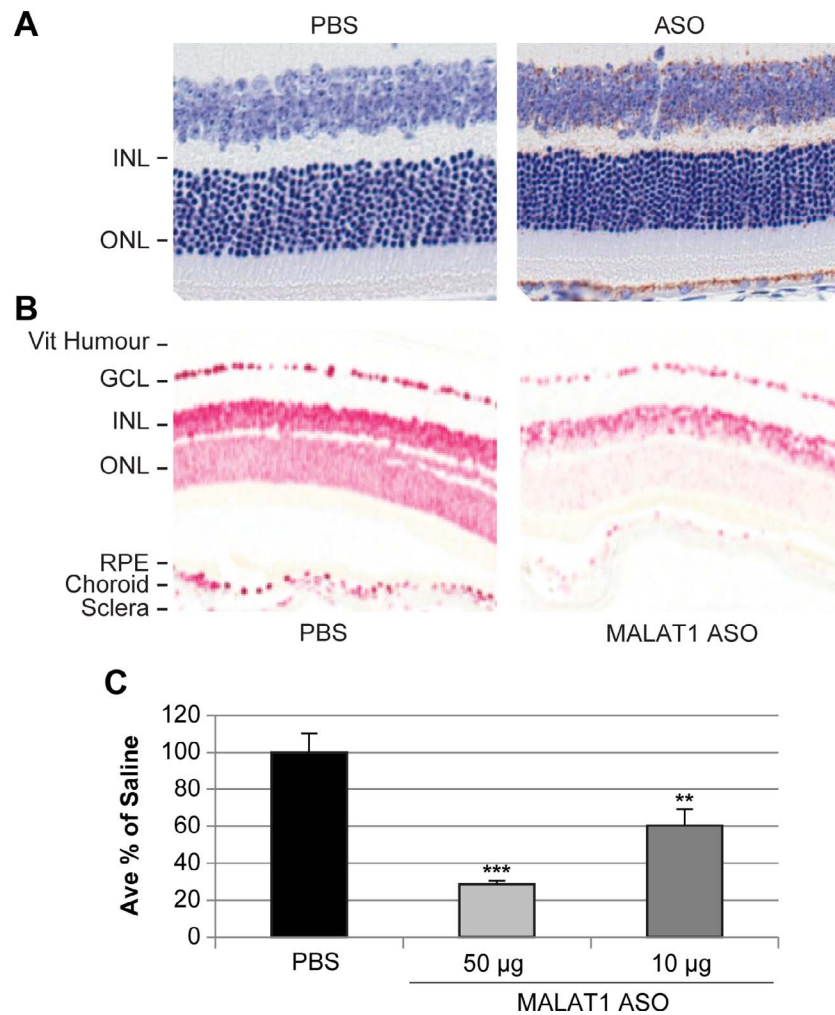
FIGURE 1. Characterization of ASO distribution and activity in mouse eyes. (**A**) Immunohistochemistry (IHC) comparison of PBS and a second generation ASO-treated mouse eyes 7 days after a 50-µg IVT injection using an anti-ASO antibody; the brown staining in the ASO eye is positive for ASO, (**B**) ISH comparison of PBS and *MALAT1* ASO (50 µg)-treated mouse eyes, and (**C**) *MALAT1* mouse mRNA expression in whole eyes 7 days after PBS, 50- or 10-µg IVT injection of the *MALAT1* ASO. RNA was normalized to ribogreen values (1-way ANOVA) All values were expressed as mean ± SD, **$P < 0.01$; ***$P < 0.001$.

by a Bonferroni multiple comparison, or a Student's 2-tailed *t*-test were performed using GraphPad Prism Version 5 (San Diego, CA, USA), software. In this report, *P* less than 0.05 was considered statistically significant.

RESULTS

ASO Distribution and Target Inhibition in the Mouse Eye Following IVT Administration

The chemical modifications of the rhodopsin ASOs used in these studies are the second generation, 2'-O-2-methoxyethyl- (MOE), modified phosphorothioate oligonucleotides, which were designed to utilize an RNaseH-dependent mechanism leading to reduction in target RNA levels.[23] ASO tissue distribution in the eye has previously been reported after injection into the rabbit eye.[27] Briefly, oligonucleotides are distributed to most of the major ocular tissues with high concentrations found in the outer plexiform layer, outer limiting membrane, inner plexiform layer, ganglion cells, ciliary body, RPE, and optic nerve. The second generation oligonucleotides are cleared very slowly from the retina, with a

half-life of approximately 2 months.[27] Given the chemical class-dependent and sequence-independent nature of ASO distribution, we expected that distribution would be similar in a rodent eye.[41,42] However, to confirm and demonstrate that ASO distributes and exhibits pharmacologic activity in all layers of a rodent eye after IVT injection, several studies were performed. First, an immunohistochemistry assay using an antibody that selectively recognizes the phosphorothioate backbone of the ASO was used to measure the presence of ASO directly.[43] The second generation ASO (50 µg) was intravitreally injected into a mouse eye and ASO distribution was evaluated 7 days post injection. No toxicities or inflammation were observed in the eyes after injection. The brown antibody staining pattern indicated distribution of ASO into all layers and was similar throughout different regions of the eye (Fig. 1A).

To demonstrate the activity of an ASO in various regions of the rodent eye, an in situ RNA hybridization assay (ISH) was used after ASO administration, as previously described.[35] A second generation ASO targeting *metastasis associated lung adenocarcinoma transcript 1* (*MALAT1*), a noncoding RNA that is ubiquitously expressed in the eye, was chosen for this analysis because of its robust signal in an ISH assay, which is a result of
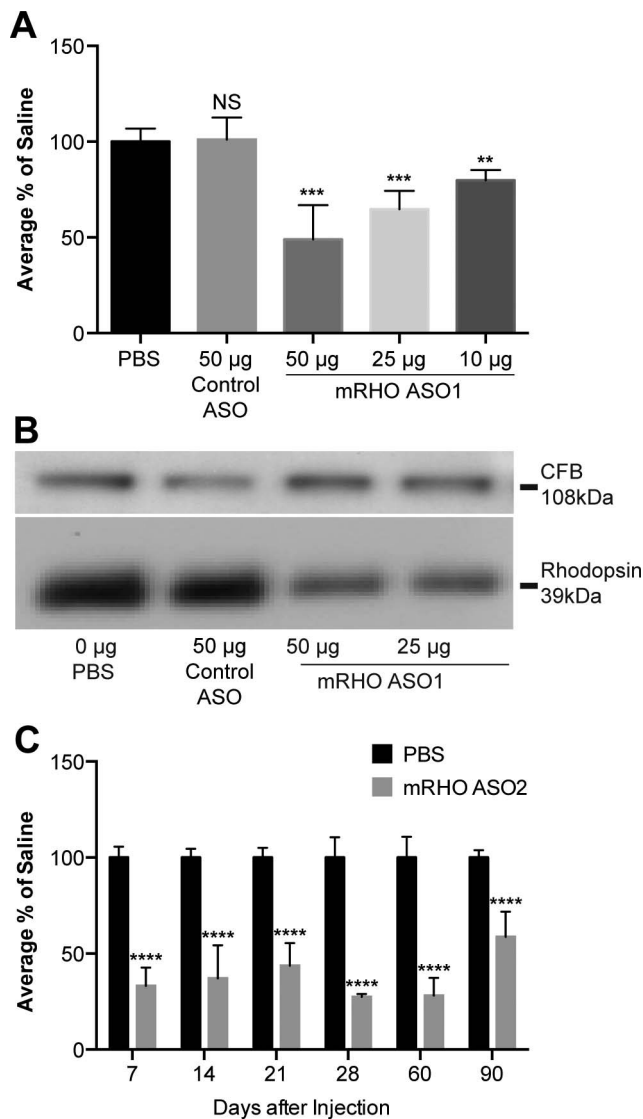
ASO Targeting Murine Rhodopsin Reduces Rhodopsin Levels in the Mouse Eye

Because the objective of the pharmacology studies in P23H-1 transgenic rats is to target the mutant mouse rhodopsin allele in the transgenic rat, the initial characterization of ASO treatment was performed in the mouse to demonstrate the in vivo efficacy of the ASOs targeting endogenous rhodopsin mRNA. First we evaluated the effects of inhibiting *rhodopsin* expression in the mouse, with a potent ASO targeting murine *rhodopsin* (mRHO ASO1) identified by screening multiple ASOs in a murine melanocyte cell line (data not shown). In vivo activity of the selected ASO was evaluated in C57BL/6 mice using qRT-PCR and Western analysis. For example, mice were treated with 50, 25, or 10 µg mRHO ASO1 or 50 µg control ASO by IVT injection and euthanized 7 days later. A dose-dependent reduction in *rhodopsin* mRNA was observed in eyes treated with mRHO ASO1, whereas no effect was observed in eyes treated with control ASO (Fig. 2A). To evaluate whether the reduction in *rhodopsin* RNA resulted in a decrease in protein levels, treated eyes ($n = 4$) were pooled and evaluated by Western blot. Protein reductions were observed in samples treated with mRHO ASO1 at both dose levels, although there did not appear to be a substantial difference in the level of reduction observed between the 50- and 25-µg doses (Fig. 2B).

Single ASO Treatment Provides a Long Duration of Action

A desired attribute of drugs given by the intravitreal route is that they be administered infrequently. In a previous study performed in rabbits, the ASO concentration in the vitreous was the highest at 3 days following a single IVT administration and declined thereafter with complete clearance from the vitreous approximately 15 days after administration, with a tissue half-life in the retina of approximately 44 days.[27] To confirm the effects observed in the photoreceptor cells with mRHO ASO1 and to accurately measure and demonstrate the duration of antisense efficacy in the rodent eye, a more active ASO was identified and used, mRHO ASO2. We measured *rhodopsin* mRNA levels at various times following a single 50-µg injection. *Rhodopsin* RNA levels in the ASO-treated mouse eye were compared with levels in the contralateral eye that received a PBS injection. Approximately a 70% reduction in *rhodopsin* RNA levels was observed over a 60-day period after a single IVT injection (Fig. 2C), demonstrating a long duration of action in the rodent eye sufficient to assess effects on ONL degeneration over extended periods post dosing.

ASO Distribution in Normal and Diseased Rat Eyes

To confirm similar ASO distribution in a normal rat eye (Fig. 3A) and the P23H-1 transgenic rat eye (Fig. 3B) the same immunohistochemistry assay used in the mouse (Fig. 1A) was performed to measure the presence of ASO directly.[43] The brown antibody staining pattern demonstrates ASO presence into all layers and was similar throughout different regions of the eye regardless of the species or disease state. Because the P23H allele in the P23H-1 line is a mouse rhodopsin gene, but the rats also express the endogenous rhodopsin, we needed to use an ASO selective for mouse versus rat rhodopsin gene. Because the two ASOs used in the mouse characterization and evaluation studies were not selective for the mouse versus rat rhodopsin sequence, a third ASO (mRHO ASO3) was identified. The mRHO ASO3 sequence used in this study has perfect complementarity to the mouse P23H *rhodopsin* gene, but has three mismatches to the rat endogenous *rhodopsin* gene in the
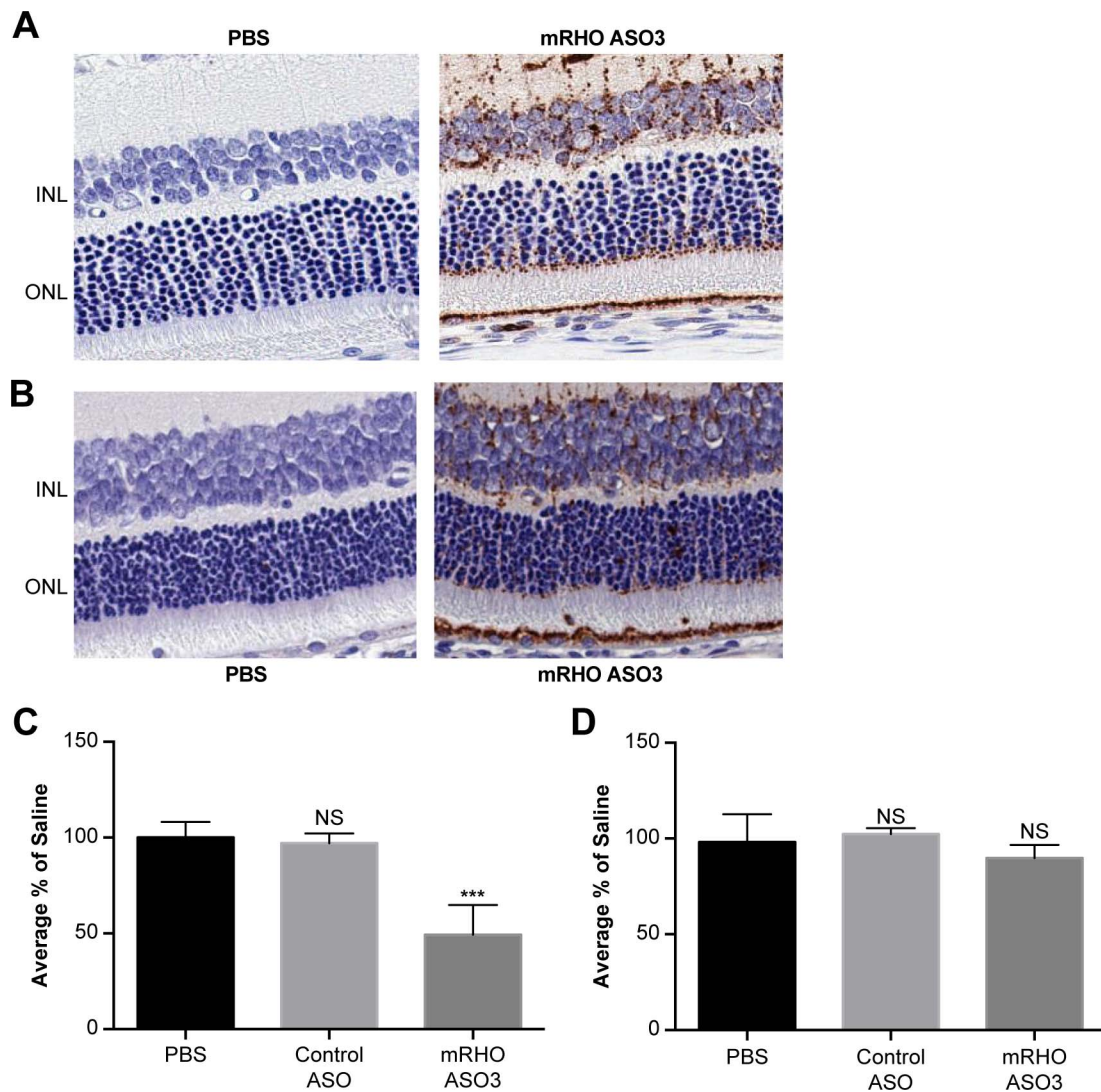

FIGURE 2. Reduction of wild-type C57BL/6 mouse *rhodopsin* expression and long duration of activity in rodent eyes after a single IVT injection of rhodopsin ASO. (**A**) Mouse *rhodopsin* mRNA expression (1-way ANOVA) and (**B**) protein expression in retina 7 days after IVT injection. (**C**) Mouse *rhodopsin* mRNA expression over time following a single 50-µg IVT injection (2-way ANOVA). All values were expressed as mean ± SD, **P < 0.01; ***P < 0.001; ****P < 0.0001. NS, no significance.

the high nuclear abundance of the RNA. The use of MALAT1 ASO allowed for analysis of activity in all ocular cell types after a single IVT injection and the nuclear localization of MALAT1 provided a strong signal for ISH analysis. This assay has been previously characterized and validated.[35] A robust reduction in *MALAT1* mRNA was observed in all layers of the eye, including the photoreceptor cells, after IVT injection of 50 µg of an ASO targeting *MALAT1* (Fig. 1B). To quantitate ASO-mediated *MALAT1* mRNA inhibition in the whole eye, mice were given IVT injections of MALAT1 ASO with doses of either 50 or 10 µg, and whole-eye RNA was evaluated by qRT-PCR 7 days later. *MALAT1* RNA levels were reduced by 71% and 40% in eyes treated with 50 and 10 µg ASO, respectively, when compared with PBS-treated eyes (Fig. 1C). These results demonstrate that following IVT administration, ASOs that distribute broadly in the rodent eye result in dose-dependent reduction of target RNA levels in most cell layers.

FIGURE 3. Characterization of ASO distribution in rat eyes and mouse specificity of the mRHO ASO3. (**A**) Immunohistochemistry comparison of PBS and mRHO ASO3-treated Sprague-Dawley rat eyes and (**B**) P23H-1 transgenic rat eyes four days after a 50-μg IVT injection using an anti-ASO antibody; the *brown staining* in the mRHO ASO3 eye is positive for ASO. (**C**) Wild-type C57BL/6 mouse *rhodopsin* mRNA expression and (**D**) wild-type Sprague-Dawley rat *rhodopsin* mRNA expression in retina 30 days after a 50-μg IVT injection (1-way ANOVA). All RNA was normalized to *cone-rod homeobox (CRX)* RNA levels. All values were expressed as mean ± SD, ***$P < 0.001$.

RNA targeted region. Hence, we evaluated the mRHO ASO3 activity for *rhodopsin* mRNA expression in wild-type C57BL/6 mice and Sprague-Dawley rats. The ASO treatment in mouse eye showed an approximately 50% reduction in *rhodopsin* RNA expression as compared with PBS-injected eyes (Fig. 3C). In contrast, no meaningful reduction in rat *rhodopsin* RNA expression was observed in the rats 30 days after a single 50 μg IVT injection as measured by qRT-PCR (Fig. 3D). The control ASO, which was designed to have no significant complementarity to known RNA sequences in the mouse or rat genomes, had no effect on levels of mouse or rat *rhodopsin* RNA.

Rhodopsin ASO Slows Photoreceptor Degeneration and Preserves Function of Photoreceptor Cells in P23H Transgenic Rat Eyes

The P23H-1 transgenic rats used in these studies undergo degeneration and photoreceptor cell loss that is generally characteristic of human P23H adRP.[30,32] The degeneration in this transgenic rat line is more aggressive than is observed in

humans, but the model provides an excellent tool for the evaluation of potential novel therapies.[30] These transgenic rats express mouse P23H mutant *rhodopsin* protein in addition to rat endogenous *rhodopsin* protein. Approximately 25% of photoreceptor cells are lost by day 15 in these animals, and there are few functional photoreceptor cells by 29 weeks of age.[30]

To evaluate the effects of P23H mouse *rhodopsin* ASO treatment on photoreceptor function in the P23H-1 transgenic rat model, ASOs were initially administered twice in order to achieve maximum target reduction, once on postnatal day 10 and again on day 21, by IVT injection. Our previous experience with double versus single IVT administration of ASOs showed a slight benefit (10%–15%) of RNA inhibition with a second injection in adult mice. Rats received PBS in their left eyes and either mRHO ASO3 or control ASO in the right eyes. On day 42 (32 days following the first injection) the rats' photoreceptor cell response was measured by ERG. The rats given mRHO ASO3 had an improved overall scotopic a-wave response and demonstrated a significantly higher maximum amplitude
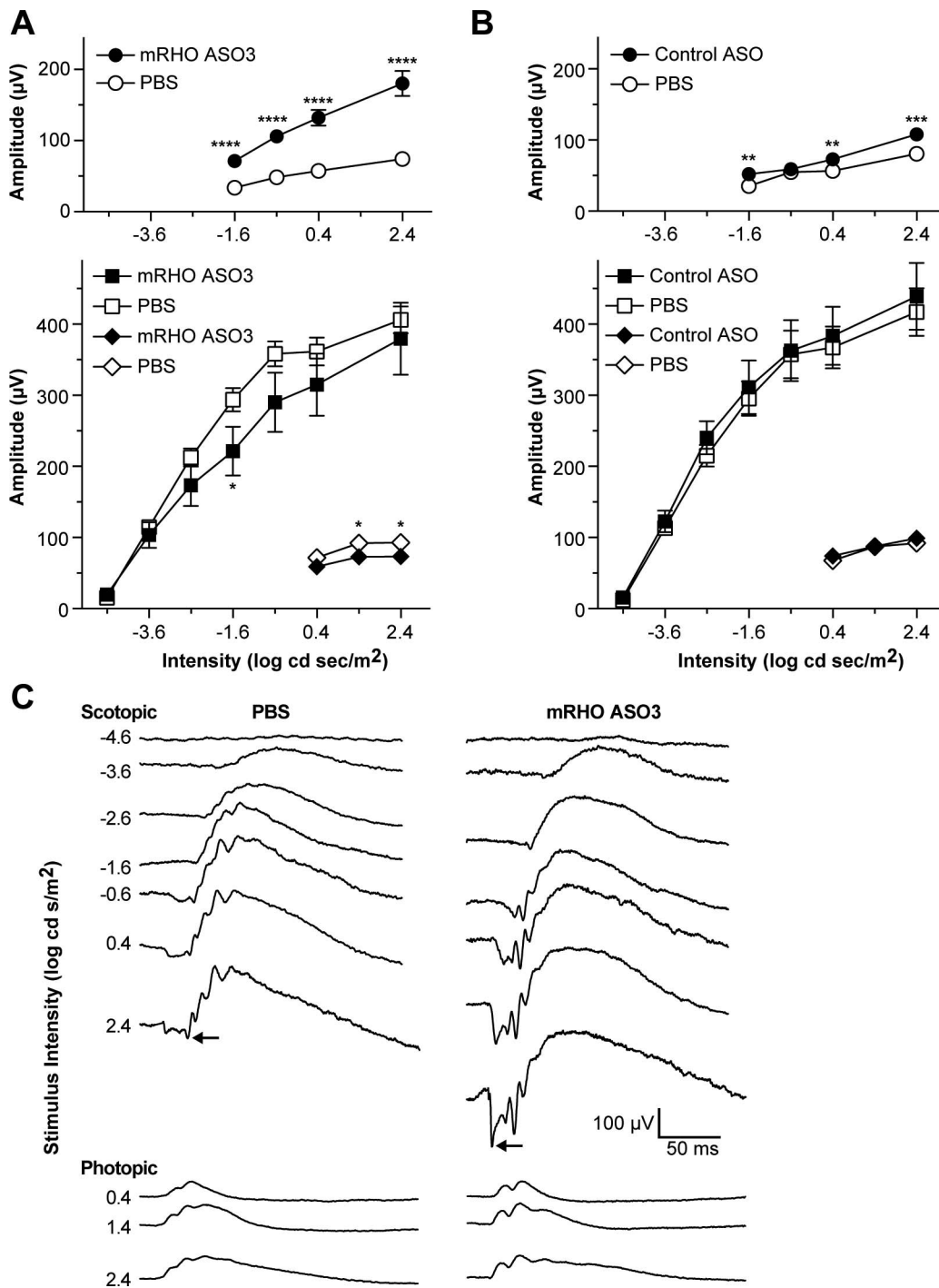
Figure 4. Improved ERG response in P23H-1 transgenic rats after mRHO ASO3 treatment with IVT injections at P10 and P21, with ERG measurements made at P42. (**A**, **B**) Amplitude versus stimulus intensity curves for scotopic a-waves (*circles*; *top panels*), scotopic b-waves (*squares*; *bottom panels*), and photopic b-waves (*diamonds*; *bottom panels*). (**A**) The scotopic a-waves of eyes injected with mRHO ASO3 were significantly greater than PBS-injected contralateral eyes, whereas the scotopic and photopic b-waves were similar to the PBS-injected eyes ($N = 21$). (**B**) Control ASO compared with PBS-injected contralateral eyes. All three of the waveforms with the control ASO were similar to those of PBS-injected contralateral eyes ($N = 7$; *t*-test; *$P < 0.05$; **$P < 0.01$; ***$P < 0.001$; ****$P < 0.0001$). In the data points without apparent *error bars*, the *error bars* are obscured by the symbol. (**C**) Representative ERG waveforms from one mouse injected with PBS in one eye (*left column*) and ASO3 in the contralateral eye (*right column*) at different stimulus intensities. As in (**A**), the mRHO ASO3-injected eye showed increasing (*downward*) a-wave amplitude (*arrows*) with increasing stimulus intensity than that of the contralateral PBS-injected eye. The waveforms of the mRho ASO3 scotopic and photopic b-waves were much more similar to those of the PBS-injected eye. The implicit time (time to peak) of the mRho ASO3-injected eye a-waves were also shorter than those of the PBS-injected eye at each stimulus intensity.
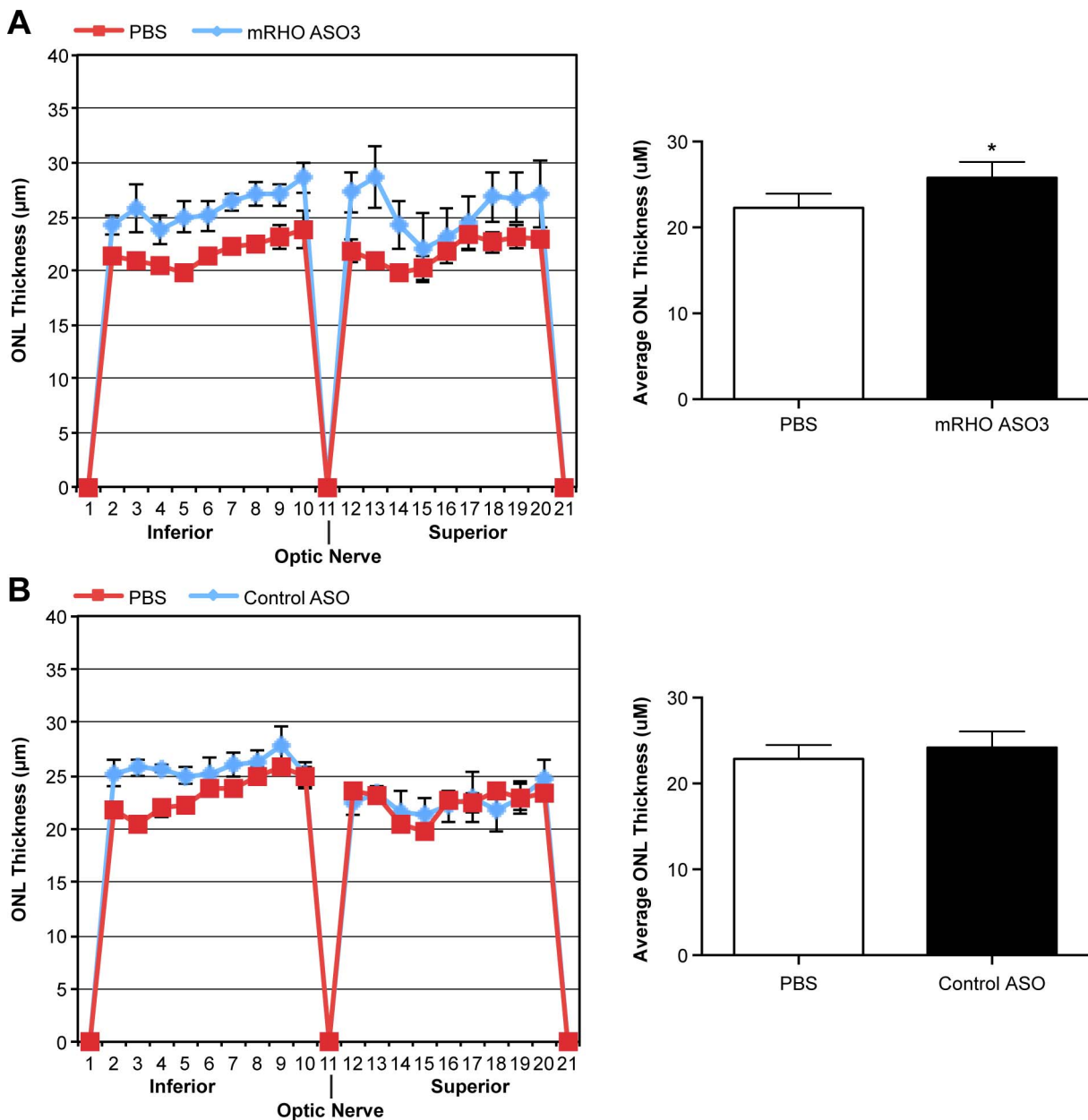
FIGURE 5. Preservation of ONL in P23H-1 transgenic rats after mRHO ASO3 treatment. (A) Spidergram of outer nuclear layer measurements of the entire retina of eyes treated with either PBS or mRHO ASO3 (*left panel*) the average thickness (±SD, *right panel*). (B) Spidergram of ONL measurements of the entire retina of PBS or Control ASO-treated eyes (*left panel*) and the average thickness (±SD, *right panel*; $N = 4$) *t*-test; *$P < 0.05$.

response (153 ± 27%) as compared with the PBS-injected contralateral eyes (Fig. 4A, top panel). Injection of mRho ASO3 improved the scotopic a-wave response amplitude at all stimulus intensities (Fig. 4A, top panel). This improved response was not observed in the control ASO-treated eyes (Fig. 4B, top panel). No significant changes were observed in the scotopic or photopic b-waves for either of the treatments (Figs. 4A, 4B, bottom panels). Four rats in the mRHO ASO3 group and four rats in the control ASO group displayed a flat ERG response presumed to be due to physical damage to the eye from the aggressive dosing protocol, so these rats were excluded from analysis.

Representative waveforms from a double-injected P23H-1 rat are shown in Figure 4C, which illustrate the significantly larger scotopic a-wave as a result of the mRHO ASO3 injections

compared with the PBS injections; the amplitudes increased with increasing stimulus intensities. As seen in the amplitude versus intensity curves (Fig. 4A), the scotopic and photopic b-waves were much more similar to the PBS-injected eye than were the scotopic a-waves at a given stimulus intensity (Fig. 4C). In addition, Figure 4C shows that mRHO ASO3 improves (shortens) the implicit time (time from stimulus to peak response) of the scotopic a-waves than that seen in the PBS-injected control eyes.

Necropsy was performed on day 45 and one-half of the eyes in each group were subjected to ONL measurements and the other half were used for RNA analysis. The mRHO ASO3-treated eyes had a thicker average ONL throughout most of the retina than that of their contralateral PBS-injected eyes (Fig. 5A). Control ASO-treated eyes had a similar ONL thickness to
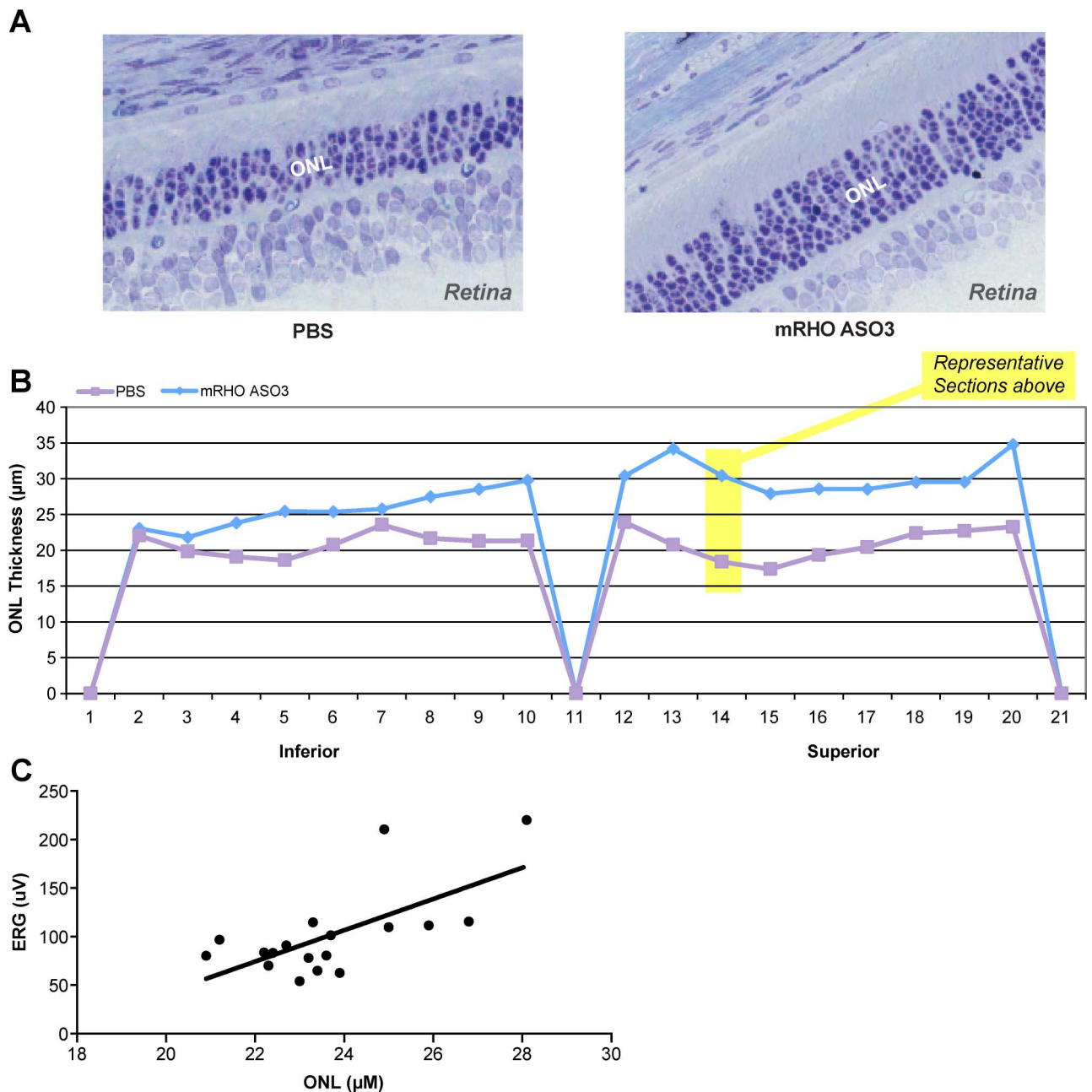
FIGURE 6. Preservation of ONL in P23H-1 transgenic rats after mRHO ASO3 treatment and correlation of ERG responses with ONL thickness. (A) Representative retinal micrographs of P23H-1 *rhodopsin* transgenic rat eyes from the PBS or mRHO ASO3-treated eye 30 days post IVT injection. (B) Spidergram profile from the same rat showing the ONL thickness throughout the retina. *Highlighted sections* show the region from which the micrographs were taken. (C) Correlation comparison of ERG amplitude responses and ONL thickness measurements ($R^2 = 0.4399$, $P < 0.0027$).

contralateral PBS-treated eyes (Fig. 5B). A representative rat was selected to visually compare an area of the contralateral PBS eye (4–6 rows) with the mRHO ASO3 eye (7–9 rows; Fig. 6A). These sections also demonstrate a consistent finding in the study that, in addition to more photoreceptor cells surviving in mRHO ASO3-injected eyes; their inner and outer segments were longer. The spidergram plot shows the sections in which the pictures were taken (Fig. 6B). All eyes that showed improvements in the ERG response also showed thicker ONL, correlating the preservation of photoreceptor cells with improved function (Fig. 6C).[44]

As mentioned above, four rats in the mRHO ASO3 group and four in the control ASO group had a flat ERG response. We

reasoned that this damage was due to injecting at an early age (on postnatal day 10) before the eyes are fully developed[29] followed by a second IVT administration 11 days later. The rationale for such an early injection was to intervene early to preserve the maximum number of photoreceptor cells; however, this approach did not take into account the vulnerability of the photoreceptor cells during the final stages of development. For this reason, a second study was carried out in which treatments were administered only once on postnatal day 14 around the time the eyes open. In these rats, the mRHO ASO3-treated eyes had an improved scotopic a-wave ERG response and the maximum amplitude was significantly greater (181 ± 39%) than that of PBS-treated eyes (Fig. 7A, top
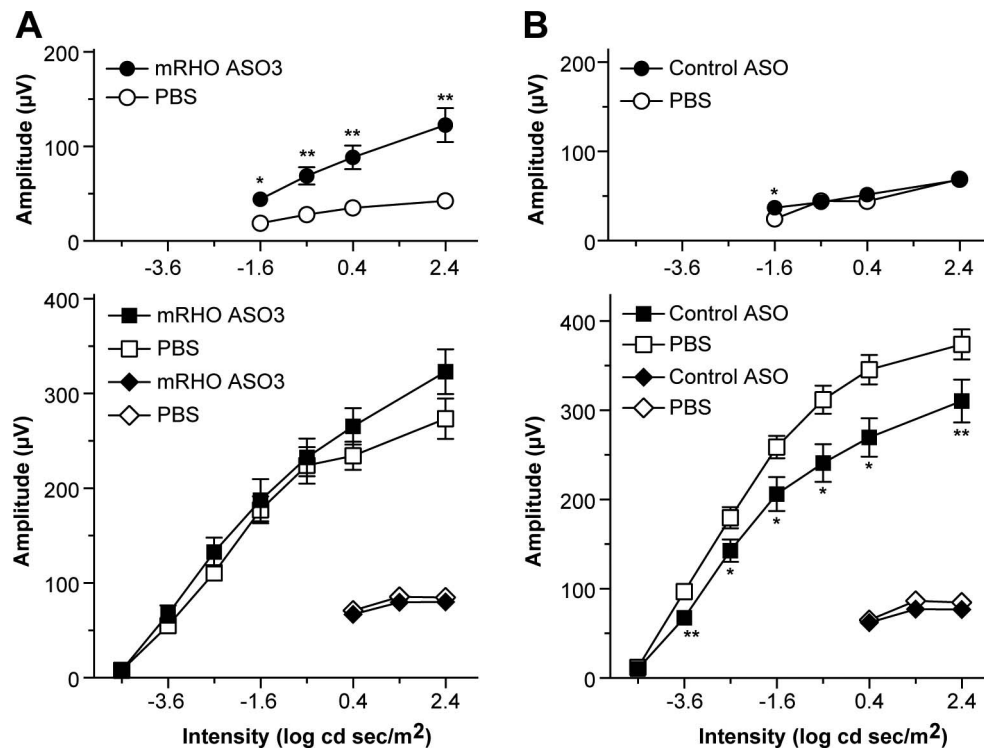
FIGURE 7. Improved ERG response in P23H-1 transgenic rats after a single mRHO ASO3 treatment with IVT injection at P13 (**A**) or P14 (**B**), with ERG measurements made at P48. (**A**, **B**) Amplitude versus stimulus intensity curves for scotopic a-waves (*circles; top panels*), scotopic b-waves (*squares; bottom panels*) and photopic b-waves (*diamonds; bottom panels*). (**A**) The scotopic a-waves of eyes injected with mRHO ASO3 were significantly greater than PBS-injected contralateral eyes, whereas the scotopic and photopic b-waves were similar to the PBS-injected eyes ($N = 10$). (**B**) Control ASO compared with PBS-injected contralateral eyes. All three of the waveforms with the control ASO were similar to those of PBS-injected contralateral eyes ($N = 10$; *t*-test; *$P < 0.05$; **$P < 0.01$). In the data points without apparent *error bars*, the *error bars* are obscured by the *symbol*.

panel), although the maximum amplitude achieved was slightly less with one injection of mRHO ASO3 than with two injections (Figs. 4A, 7A, top panels). Moreover, no flat ERG responses were observed with a single injection. Again, no significant effects were observed on the scotopic or photopic b-wave after treatment (Fig. 7A, bottom panel). The control ASO eyes did not differ significantly in any of the ERG responses from those of PBS-treated eyes (Figs. 7A, 7B). Thus, the amplitude responses after ASO treatment in this study were similar to those observed in the previous study with two injections, but no negative effects were observed. Apparently the slight benefit (greater a-wave amplitude) gained from a second dose did not outweigh the potential damage of deleterious effects from a second intervention given shortly after the first injection (11 days) in these young animals.

Eyes from this study were also evaluated for rat and mouse *rhodopsin* mRNA expression. Rat *rhodopsin* expression was higher for individual rats that had a 100% or greater ERG response in the mRHO ASO3 group as compared with their PBS-injected contralateral eye (Fig. 8A) indicating preservation of photoreceptor cells. By contrast, an increase in rat RHO expression was not observed in any of the control ASO-treated rats, indicating a lack of photoreceptor cell preservation (Fig. 8B). Similar to the ONL thickness correlation with ERG, rats that showed better ERG response were highly correlated with levels of rat *rhodopsin* mRNA (Fig. 8C).

To determine the amount of mouse P23H *rhodopsin* reduction achieved by ASO treatment, we dosed a separate group of transgenic rats ($n = 19$) on day 16 with a single 50 μg IVT injection of mRHO ASO3 and euthanized them 4 days later. This time point was necessary because of confounding effects

caused by (1) rapid degeneration of the photoreceptor cells over time, and (2) the inhibition of degeneration achieved by the treatment in the mRHO ASO3 injected eyes makes it inappropriate to compare with their PBS contralateral eye with longer time points. We observed a significant reduction in mouse *rhodopsin* RNA in the ASO-treated eye (averaging $30 \pm 5\%$) and no significant reduction in rat *rhodopsin* RNA (averaging $\sim 2 \pm 5\%$) as compared with their respective PBS-treated eye by *qRT-PCR* (Fig. 8D), confirming the allele specificity that was observed in normal animals. Additionally, four treated eyes from the transgenic rats were fixed in Davidson's solution and an in situ RNA hybridization assay (ISH) was used to visualize the mRHO ASO3 activity specifically against mutant murine *rhodopsin* mRNA expression (Fig. 8E). In situ RNA hybridization assay analysis of rhodopsin RNA levels demonstrated a similar reduction of RNA expression in the ASO-treated eye as compared with qRT-PCR.

DISCUSSION

In this report, we demonstrated that IVT administration of ASO can lower *rhodopsin* levels in a rodent eye. These effects were observed upon IVT injection of ASO dissolved in a simple water-based solution; thus, there was no need for a complex delivery system. In addition, the ASO distributed broadly into all layers in the eye and exhibited a long duration of action. In a rabbit eye the half-life of second generation ASOs was calculated to be approximately 44 days[27] in the retina supporting a long duration of action. This indicates that patients could be dosed quarterly or even less frequently. Furthermore, the ASO approach for ocular diseases has been
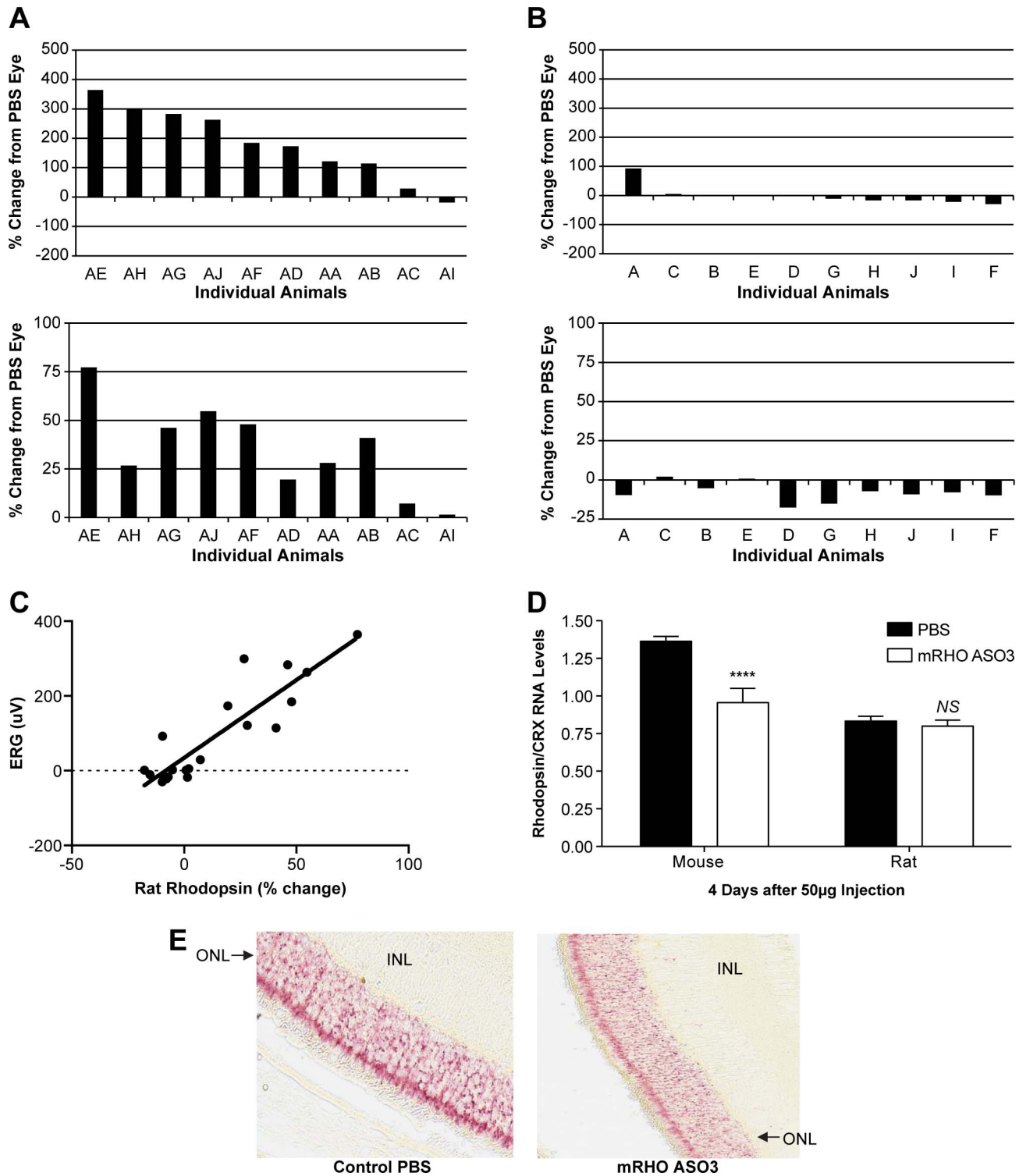
FIGURE 8. mRHO ASO treatment preserved rat *rhodopsin* expression, which correlates with better ERG response in P23H transgenic rats after a single IVT injection. The percentage change in scotopic a-wave amplitude response (*top*) or rat endogenous *rhodopsin* RNA levels (*bottom*) from the eyes of the individual animals treated with (**A**) mRHO ASO3 compared with their contralateral PBS treated eye or (**B**) control ASO compared with their contralateral PBS eye, 0% indicates no change. (**C**) Correlation comparison of ERG amplitude response and the percentage change in the endogenous rat *rhodopsin* RNA levels ($R^2 = 0.798$, $P < 0.0001$). (**D**) Mouse and rat *rhodopsin* mRNA expression normalized to rat *CRX* ($n = 19$) and (**E**) representative histology image from ISH comparison of PBS and mRHO ASO3-treated mouse eyes 4 days after a 50-µg IVT injection administered on postnatal day 16 in the P23H transgenic rat Line 1. All values were expressed as mean ± SEM, *t*-test, ****$P < 0.0001$.

clinically validated, with the Food and Drug Administration approval of Vitravene (Isis Pharmaceuticals, Carlsbad, CA, USA and Novartis Ophthalmics AG, Bulach, Switzerland), a first generation ASO developed for the treatment of cytomegalovirus (CMV) retinitis.[25,28] Additionally, the second generation ASO chemistry used in this study offers an improved profile relative to first generation ASO chemistry with respect to potency, duration of action, and overall tolerability.[27] Since the P23H transgenic line we used in these studies was rat, but the targeted mutant rhodopsin gene was mouse, we needed to demonstrate activity in one species and pharmacology effects in another. Fortunately, the properties of antisense oligonucleotides are such that the pharmacokinetics of phosphorothioate oligonucleotides are independent of sequence and that the pattern of distribution to organs and across specific cell types is similar across species as demonstrated by Geary et al.[41] The correlation between species provides a level of confidence when translating ASO activity from one species to another as long as the target gene sequence is the same, as is the case in a transgenic animal model.

In these present studies, we demonstrated that ASO treatment against murine rhodopsin mRNA containing the P23H mutation can slow the rate of degeneration of photoreceptor cells in a rat model of adRP using an antisense inhibitor designed to selectively reduce the mutant murine rhodopsin allele. Both the photoreceptor cell structure and function were preserved 30 days following mRHO ASO treatment in the P23H-1 transgenic rat as indicated by a thicker ONL and greater ERG a-wave maximum responses, compared with contralateral control eyes. In an extensive ERG study of P23H-1 rats, Machida et al.[30] concluded that the scotopic a-wave maximum amplitude appears to be a better parameter than the b-wave to judge efficacy of therapeutic manipulation of this rat model of retinal disease. The scotopic b-wave remained nearly constant in P23H-1 rats despite of the loss of photoreceptors over a period of 29 weeks.[30] Thus, it is not surprising in our study that while the a-wave showed a significant improvement from mRHO ASO3 treatment, the b-wave showed none. Similarly, the lack of improvement of the cone-dominated photopic b-wave response is not surprising given the status of the photopic ERG in P23H-1 rats at their age in the present studies. Machida et al.[30] found that "the photopic ERG was normal at 4 weeks and began to decline by 8 weeks of age." In the present studies, the eyes were injected around 2 weeks of age (at either P10 or P14), and then studied at just less than 7 weeks of age. Thus, for most of the experimental period, the photopic b-wave was indistinguishable from that in normal rats, so little or no improvement would be expected.

The maximal scotopic a-wave responses from ASO-treated eyes were approximately 150% to 180% greater than those from contralateral control eyes. To understand the therapeutic potential of the ASO treatment, the a-wave amplitudes would ideally be compared with those of normal, age-matched wild-type Sprague-Dawley rats, but no such contemporaneously measured ERGs were available. To make an approximate comparison, we used the maximal scotopic a-wave response amplitudes of wild-type Sprague-Dawley rats close to the age examined in the present experiments as measured in four different laboratories, including our own; this average value was 410 μV (450 μV, fig. 3A in Machida et al.[30]; 390 μV, calculated from text and fig. 1A in Wong et al.[45]; 415 μV, fig. 4B in Orhan et al.[34]; 385 μV, LaVail MM, Nielsen GK, Matthes MT, unpublished observations, 2011). Thus, the maximal scotopic a-wave amplitude resulting from two ASO injections (Fig. 4) was approximately 175 μV, or approximately 43% of that in wild-type animals. The response from the single ASO injections (Fig. 7) was approximately 120 μV, or approximately 29% of

that in wild-type animals. These are relatively high percentages of normal when the very rapid, aggressive rate of photoreceptor degeneration is considered. Presumably, the relative degree of ASO-mediated protection would be greater with a milder, slower retinal degeneration, but this remains to be determined experimentally with both a slower degeneration model and contemporaneously measured wild-type controls. This would also allow a better understanding of ASO treatment on scotopic and photopic b-wave responses and implicit times than in the rapid P23H-1 retinal degeneration model.

This is the first demonstration of an oligonucleotide-based inhibitor delivered directly into the eye that preserves photoreceptor cell structure and function in an animal model that is reflective of the disease in humans. Although studies have been reported demonstrating allele-selective rescue of photoreceptor cells in the P23H transgenic Line 3,[20] which has a slower rate of degeneration and a less severe phenotype than the transgenic line 1 used in this study, those earlier reports used an AAV-mediated ribozyme injected subretinally.[22] Since wild-type rhodopsin expression is necessary for preservation of photoreceptor cell function, effective gene-based therapeutic approaches must preferentially inhibit mutant rhodopsin while preserving normal rhodopsin expression, or therapy must include a replacement of the wild-type protein. In dominant negative diseases, such as P23H adRP, data suggest that significant phenotypic improvements can result from modest reductions in the mutant protein when wild-type protein expression is preserved.[20,21] Characterization of several different lines of transgenic animals and affected adRP patients demonstrate a negative correlation of normal to mutant rhodopsin expression with disease severity.[46,47] In addition, it has been demonstrated that increasing expression of normal rhodopsin in animal models of adRP results in a slower rate of degeneration of the photoreceptor cells and preservation of vision for longer periods of time.[47,48] Here, we achieved a 30% reduction in mutant rhodopsin expression and no reduction in the normal rat rhodopsin expression through allele-specific antisense targeting. This reduction results in an increase in the amount of normal to mutant rhodopsin expression supporting a slower rate of photoreceptor degeneration as demonstrated by ONL and ERG analyses.

An ideal treatment for adRP diseases would be an allele-selective therapeutic that prevents expression of the diseased allele, while maintaining expression of the wild-type variant. Oligonucleotide-based therapeutics are uniquely suited for targeting autosomal genetic diseases, as these agents can suppress the production of the mutant protein while preserving the wild-type protein by targeting the mRNA directly through Watson-Crick interactions.[23,49] Furthermore, ASOs can provide substantial activity in targeting a single base point mutation, while preserving the wild-type allele using optimized ASO designs.[26] In the clinic, it will be necessary to use such an ASO that demonstrates selectivity for the mutant allele having a single nucleotide change.

In conclusion, allele-selective targeting of mutant rhodopsin resulted in improved photoreceptor cell preservation and cell viability in a rat model of a dominant negative retinal degenerative disease.

Acknowledgments

References

1. Bird AC. Retinal photoreceptor dystrophies LI. Edward Jackson Memorial Lecture. *Am J Ophthalmol*. 1995;119:543–562.

2. Boughman JA, Conneally PM, Nance WE. Population genetic studies of retinitis pigmentosa. *Am J Hum Genet*. 1980;32:223–235.

3. Schuster A, Weisschuh N, Jagle H, et al. Novel rhodopsin mutations and genotype-phenotype correlation in patients with autosomal dominant retinitis pigmentosa. *Br J Ophthalmol*. 2005;89:1258–1264.

4. Sullivan LS, Bowne SJ, Birch DG, et al. Prevalence of disease-causing mutations in families with autosomal dominant retinitis pigmentosa: a screen of known genes in 200 families. *Invest Ophthalmol Vis Sci*. 2006;47:3052–3064.

5. Wang DY, Chan WM, Tam PO, et al. Gene mutations in retinitis pigmentosa and their clinical implications. *Clin Chim Acta*. 2005;351:5–16.

6. Dryja TP, Hahn LB, Cowley GS, McGee TL, Berson EL. Mutation spectrum of the rhodopsin gene among patients with autosomal dominant retinitis pigmentosa. *Proc Natl Acad Sci U S A*. 1991;88:9370–9374.

7. Dryja TP, McGee TL, Reichel E, et al. A point mutation of the rhodopsin gene in one form of retinitis pigmentosa. *Nature*. 1990;343:364–366.

8. LaVail MM, Yasumura D, Matthes MT, et al. Protection of mouse photoreceptors by survival factors in retinal degenerations. *Invest Ophthalmol Vis Sci*. 1998;39:592–602.

9. Chadderton N, Millington-Ward S, Palfi A, et al. Improved retinal function in a mouse model of dominant retinitis pigmentosa following AAV-delivered gene therapy. *Mol Ther*. 2009;17:593–599.

10. O'Reilly M, Palfi A, Chadderton N, et al. RNA interference-mediated suppression and replacement of human rhodopsin in vivo. *Am J Hum Genet*. 2007;81:127–135.

11. Mendes HF, Cheetham ME. Pharmacological manipulation of gain-of-function and dominant-negative mechanisms in rhodopsin retinitis pigmentosa. *Hum Mol Genet*. 2008;17:3043–3054.

12. Rossmiller B, Mao H, Lewin AS. Gene therapy in animal models of autosomal dominant retinitis pigmentosa. *Mol Vis*. 2012;18:2479–2496.

13. Gorbatyuk M, Justilien V, Liu J, Hauswirth WW, Lewin AS. Preservation of photoreceptor morphology and function in P23H rats using an allele independent ribozyme. *Exp Eye Res*. 2007;84:44–52.

14. Gorbatyuk MS, Pang JJ, Thomas J Jr, Hauswirth WW, Lewin AS. Knockdown of wild-type mouse rhodopsin using an AAV vectored ribozyme as part of an RNA replacement approach. *Mol Vis*. 2005;11:648–656.

15. Kiang AS, Palfi A, Ader M, et al. Toward a gene therapy for dominant disease: validation of an RNA interference-based mutation-independent approach. *Mol Ther*. 2005;12:555–561.

16. Mussolino C, Sanges D, Marrocco E, et al. Zinc-finger-based transcriptional repression of rhodopsin in a model of dominant retinitis pigmentosa. *EMBO Mol Med*. 2011;3:118–128.

17. Asokan A, Schaffer DV, Samulski RJ. The AAV vector toolkit: poised at the clinical crossroads. *Mol Ther*. 2012;20:699–708.

18. Mao H, James T Jr, Schwein A, et al. AAV delivery of wild-type rhodopsin preserves retinal function in a mouse model of autosomal dominant retinitis pigmentosa. *Hum Gene Ther*. 2011;22:567–575.

19. Drenser KA, Timmers AM, Hauswirth WW, Lewin AS. Ribozyme-targeted destruction of RNA associated with autosomal-dominant retinitis pigmentosa. *Invest Ophthalmol Vis Sci*. 1998;39:681–689.

20. LaVail MM, Yasumura D, Matthes MT, et al. Ribozyme rescue of photoreceptor cells in P23H transgenic rats: long-term survival and late-stage therapy. *Proc Natl Acad Sci U S A*. 2000;97:11488–11493.

21. Gorbatyuk M, Justilien V, Liu J, Hauswirth WW, Lewin AS. Suppression of mouse rhodopsin expression in vivo by AAV mediated siRNA delivery. *Vision Res*. 2007;47:1202–1208.

22. Lewin AS, Drenser KA, Hauswirth WW, et al. Ribozyme rescue of photoreceptor cells in a transgenic rat model of autosomal dominant retinitis pigmentosa. *Nat Med*. 1998;4:967–971.

23. Bennett CF, Swayze EE. RNA targeting therapeutics: molecular mechanisms of antisense oligonucleotides as a therapeutic platform. *Annu Rev Pharmacol Toxicol*. 2010;50:259–293.

24. Gregory E Hardee LGT, Geary. Richard S. Routes and formulations for delivery of antisense oligonucleotides. In: Crooke ST, ed. *Antisense Drug Technology: Principles, Strategies, and Applications*. Boca Raton, FL: CRC Press, Taylor and Francis Group; 2008:217–236.

25. Kwoh TJ. An overview of the clinical safety experience of first- and second-generation antisense oligonucleotides. In: Crooke ST, ed. *Antisense Drug Technology: Principles, Strategies, and Applications*. Boca Raton, FL: CRC Press, Taylor and Group Francis; 2008:365–399.

26. Ostergaard ME, Southwell AL, Kordasiewicz H, et al. Rational design of antisense oligonucleotides targeting single nucleotide polymorphisms for potent and allele selective suppression of mutant Huntingtin in the CNS. *Nucleic Acids Res*. 2013;41:9634–9650.

27. Henry SP, Miner RC, Drew WL, et al. Antiviral activity and ocular kinetics of antisense oligonucleotides designed to inhibit CMV replication. *Invest Ophthalmol Vis Sci*. 2001;42:2646–2651.

28. Vitravene Study G. Safety of intravitreous fomivirsen for treatment of cytomegalovirus retinitis in patients with AIDS. *Am J Ophthalmol*. 2002;133:484–498.

29. Lee D, Geller S, Walsh N, et al. Photoreceptor degeneration in Pro23His and S334ter transgenic rats. *Adv Exp Med Biol*. 2003;533:297–302.

30. Machida S, Kondo M, Jamison JA, et al. P23H rhodopsin transgenic rat: correlation of retinal function with histopathology. *Invest Ophthalmol Vis Sci*. 2000;41:3200–3209.

31. Cuenca N, Pinilla I, Sauve Y, Lu B, Wang S, Lund RD. Regressive and reactive changes in the connectivity patterns of rod and cone pathways of P23H transgenic rat retina. *Neuroscience*. 2004;127:301–317.

32. Berson EL, Rosner B, Sandberg MA, Dryja TP. Ocular findings in patients with autosomal dominant retinitis pigmentosa and a rhodopsin gene defect (Pro-23-His). *Arch Ophthalmol*. 1991;109:92–101.

33. Seth PP, Vasquez G, Allerson CA, et al. Synthesis and biophysical evaluation of $2',4'$-constrained $2'$O-methoxyethyl and $2',4'$-constrained $2'$O-ethyl nucleic acid analogues. *J Org Chem*. 2010;75:1569–1581.

34. Orhan EDD, Neuille M, Lechauve C, et al. Genotypic and phenotypic characterization of P23H Line 1 rat model. *PLoS One*. 2015;10:e0127319.

35. Hung G, Xiao X, Peralta R, et al. Characterization of target mRNA reduction through in situ RNA hybridization in multiple organ systems following systemic antisense treatment in animals. *Nucleic Acid Ther*. 2013;23:369–378.

36. Kordasiewicz HB, Stanek LM, Wancewicz EV, et al. Sustained therapeutic reversal of Huntington's disease by transient repression of huntingtin synthesis. *Neuron*. 2012;74:1031–1044.

37. Bayer AU, Mittag T, Cook P, Brodie SE, Podos SM, Maag KP. Comparisons of the amplitude size and the reproducibility of three different electrodes to record the corneal flash electroretinogram in rodents. *Doc Ophthalmol*. 1999;98:233–246.

38. LaVail MM, Battelle BA. Influence of eye pigmentation and light deprivation on inherited retinal dystrophy in the rat. *Exp Eye Res*. 1975;21:167–192.

39. Faktorovich EG, Steinberg RH, Yasumura D, Matthes MT, LaVail MM. Photoreceptor degeneration in inherited retinal dystrophy delayed by basic fibroblast growth factor. *Nature*. 1990;347:83–86.

40. Michon JJ, Li ZL, Shioura N, Anderson RJ, Tso MO. A comparative study of methods of photoreceptor morphometry. *Invest Ophthalmol Vis Sci*. 1991;32:280–284.

41. Geary RS, Leeds JM, Henry SP, Monteith DK, Levin AA. Antisense oligonucleotide inhibitors for the treatment of cancer: 1. Pharmacokinetic properties of phosphorothioate oligodeoxynucleotides. *Anticancer Drug Des*. 1997;12:383–393.

42. Yu RZ, Grundy JS, Geary RS. Clinical pharmacokinetics of second generation antisense oligonucleotides. *Expert Opin Drug Metab Toxicol*. 2013;9:169–182.

43. Butler M, Stecker K, Bennett CF. Cellular distribution of phosphorothioate oligodeoxynucleotides in normal rodent tissues. *Lab Invest*. 1997;77:379–388.

44. Wen Y, Klein M, Hood DC, Birch DG. Relationships among multifocal electroretinogram amplitude, visual field sensitivity, and SD-OCT receptor layer thicknesses in patients with retinitis pigmentosa. *Invest Ophthalmol Vis Sci*. 2012;53:833–840.

45. Wong LL, Pye QN, Chen L, Seal S, McGinnis JF. Defining the catalytic activity of nanoceria in the P23H-1 rat, a photoreceptor degeneration model. *PLoS One*. 2015;10:e0121977.

46. Frederick JM, Krasnoperova NV, Hoffmann K, et al. Mutant rhodopsin transgene expression on a null background. *Invest Ophthalmol Vis Sci*. 2001;42:826–833.

47. Olsson JE, Gordon JW, Pawlyk BS, et al. Transgenic mice with a rhodopsin mutation (Pro23His): a mouse model of autosomal dominant retinitis pigmentosa. *Neuron*. 1992;9:815–830.

48. Price BA, Sandoval IM, Chan F, et al. Rhodopsin gene expression determines rod outer segment size and rod cell resistance to a dominant-negative neurodegeneration mutant. *PLoS One*. 2012;7:e49889.

49. O'Connor TP, Crystal RG. Genetic medicines: treatment strategies for hereditary disorders. *Nat Rev Genet*. 2006;7:261–276.